EurJIC
European Journal of Inorganic Chemistry

Full Papers
doi.org/10.1002/ejic.202100079

Chemistry Europe
European Chemical Societies Publishing

Bis(8-hydroxyquinoline) Ligands: Exploring their Potential as Selective Copper-Binding Agents for Alzheimer's Disease

Valentina Oliveri*[a] and Graziella Vecchio[a]

Amyloid-β (Aβ) aggregation, metal ion dyshomeostasis, and oxidative stress are pathological features of Alzheimer's disease (AD). Aβ and metal ions form metal-Aβ complex species that influence the aggregation of Aβ and, in particular, redox metal ions such as Cu lead to the production of reactive oxygen species (ROS). To target metal coordination to Aβ and the reactivities of Cu–Aβ, metal chelating agents must extract Cu^{2+} from Aβ in AD pathological conditions. Bis(8-hydroxyquinoline) ligands can extract Cu^{2+} from Aβ and therefore inhibit the Cu-induced Aβ aggregation and the aerobic oxidation of ascorbate. In particular, N-butyl-2,2-imino-bis(8-hydroxyquinoline) can selectively target Cu–Aβ reactivities in the presence of Zn^{2+} such as in AD brain patients. The ligands can release Cu in intracellular environments in the presence of a large excess of glutathione, contributing to restore Cu homeostasis.

Introduction

Patients with neurodegenerative diseases (NDs) are increasing across the globe, as a consequence of the extension of life expectancy. Therefore, NDs are a major health problem worldwide.[1,2]

Common central elements in the etiology of NDs are the aggregation of intrinsically disordered proteins and oxidative stress due to the overproduction of reactive oxygen species (ROS).[3,4] Both these phenomena are affected or triggered by transition metal ions.[5] Cu^{2+} and Zn^{2+} influence the aggregation of amyloid-β (Aβ) and α-synuclein in Alzheimer's disease (AD) and Parkinson's disease, respectively.[6–8] This evidence has led to the investigation of metal-binding agents as drug candidates for the treatment of neurodegenerative disorders.[9,10]

In particular, AD is a multifactorial and complex disease where oxidative stress, Aβ clearance dysfunctions, Aβ and tau aggregation, and metal ions dyshomeostasis play a prominent role in disease etiology. The Aβ peptide binds Cu^{2+} and Zn^{2+} in the N-terminal region, exhibiting a Cu^{2+} over Zn^{2+} selectivity of 2–3 orders of magnitude.[5,11] The levels of metal ions in senile plaques are higher compared to age-matched non-AD controls, and the interaction between metal ions and the Aβ peptide drastically affects the Aβ aggregation process.[12,13] Moreover, Cu bound to extracellular Aβ catalyzes the incomplete reduction of dioxygen leading to hydroxyl radical and other ROS species, which cause severe oxidative damage with permanent modification of neurotransmitters, cellular lipids, nucleic acids, and proteins.[5],[14]

Notwithstanding zinc ions are more abundant than copper ions in the synaptic cleft, its redox inertness and the low propensity for Aβ make them less harmful than redox competent Cu ions.[14,15] The need for selectivity between Cu and Zn ions has emerged in the field of the chelation therapy[16,17] and Hureau's group has recently addressed this issue in AD.[18–20]

In this context, Cu homeostasis is considered a valuable target in AD treatment,[21,22] and the possibility of using metal chelators or ionophores to regenerate metal homeostasis and then inhibit the progressive neurodegeneration is largely studied.[22,23] The proposed metal chelators for the treatment of AD has been extensively reviewed elsewhere.[9,24] Among them, the family of chelating 8-substituted quinoline has received wide research attention. Clioquinol and PBT2, two non-specific Cu–Zn ionophores, showed to improve learning and memory capacities of APP transgenic mice.[25,26] Nevertheless, they failed to achieve neuroprotection in clinical trials.[27] However, the in vitro and in vivo results have propelled the development of other chelating 8-substituted quinoline with higher selectivity for copper or with multiple biological activities to hit multiple targets.[10,28–30] Recently, we focused on the study and development of 8-hydroxyquinoline (HQ) derivatives;[31–33] in particular, we derivatized HQ scaffold with different moieties (saccharides, peptides) to confer it different anti-neurodegenerative functions.[34–36] Meunier and coworkers have developed tetradentate derivatives of bis(8-aminoquinolines), including PA1637, demonstrating that these compounds outperform HQs (such as clioquinol and PBT2).[37,38] Moreover, it has been reported that N_4-tetradentate ligands inhibit the aerobic oxidation of ascorbate induced by Cu–$A\beta_{16}$ in a Zn-rich environment.[39] The authors, comparing different chelators with N_4, N_2O_2, and N_3O_2 coordination sphere, conclude that chelators should exhibit an N_4-tetradentate motif to selectively target Cu and inhibit the ROS production caused by Cu-bound Aβ

[a] Dr. V. Oliveri, Prof. G. Vecchio
Dipartimento di Scienze Chimiche
Università degli Studi di Catania
viale A. Doria 6, 95125,
Catania, Italy
E-mail: valentina.oliveri@unict.it

Supporting information for this article is available on the WWW under https://doi.org/10.1002/ejic.202100079

species.[39] Here, we demonstrate that the N_4-tetradentate motif is not crucial for the selective extraction of Cu from Aβ species.

In particular, we evaluated the ability of two N_2O_2 bis(8-hydroxyquinoline) ligands (bisHQs, Figure 1) to affect Cu-induced amyloid aggregation and the ROS production of Cu–Aβ species, to extract Cu from Cu–Aβ species and release Cu in the presence of GSH. These investigations were also performed in the presence of Zn^{2+} ions to mimic the brain environment of AD. The bisHQs reported in Figure 1 were selected for their anti-AD properties such as the ability to interact with Aβ, the inhibition of fibrillar amyloid aggregation, and the capacity to scavenge free radical species.[40] These properties can be linked to the (poly)-aromatic system, OH phenolic groups, and in the case of $Tre(HQ)_2$ to the presence of the sugar moiety.[21,41,42]

Here, we investigated if they can also target another significant aspect of NDs: the Cu dyshomeostasis.

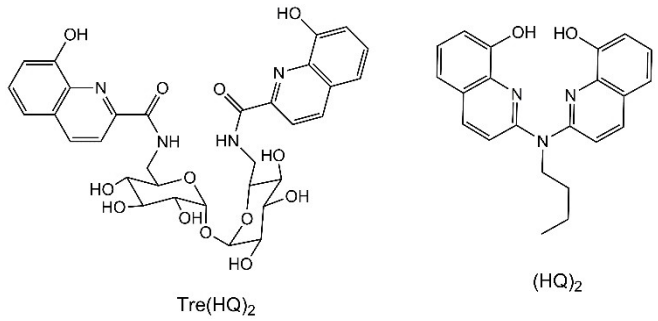

Figure 1. Structures of the bis(8-hydroxyquinoline) ligands: 6,6′-dideoxy-6,6′-di[(8-hydroxyquinoline)-2-carboxyl]amino]-α,α′-trehalose ($Tre(HQ)_2$), N-butyl-2,2-imino-bis(8-hydroxyquinoline) ($(HQ)_2$).

Results and Discussion

Copper and zinc complexes. The ability of $Tre(HQ)_2$ and $(HQ)_2$ to chelate Cu^{2+} and Zn^{2+} was monitored by UV-vis, CD titration, and ESI-mass spectrometry (Figure 2, Figures S1–S10, Table S1). As for $Tre(HQ)_2$, spectral CD and UV modifications are significant upon the addition of aliquots of concentrated aqueous solutions of Cu^{2+} and Zn^{2+}, indicating the metal complexation

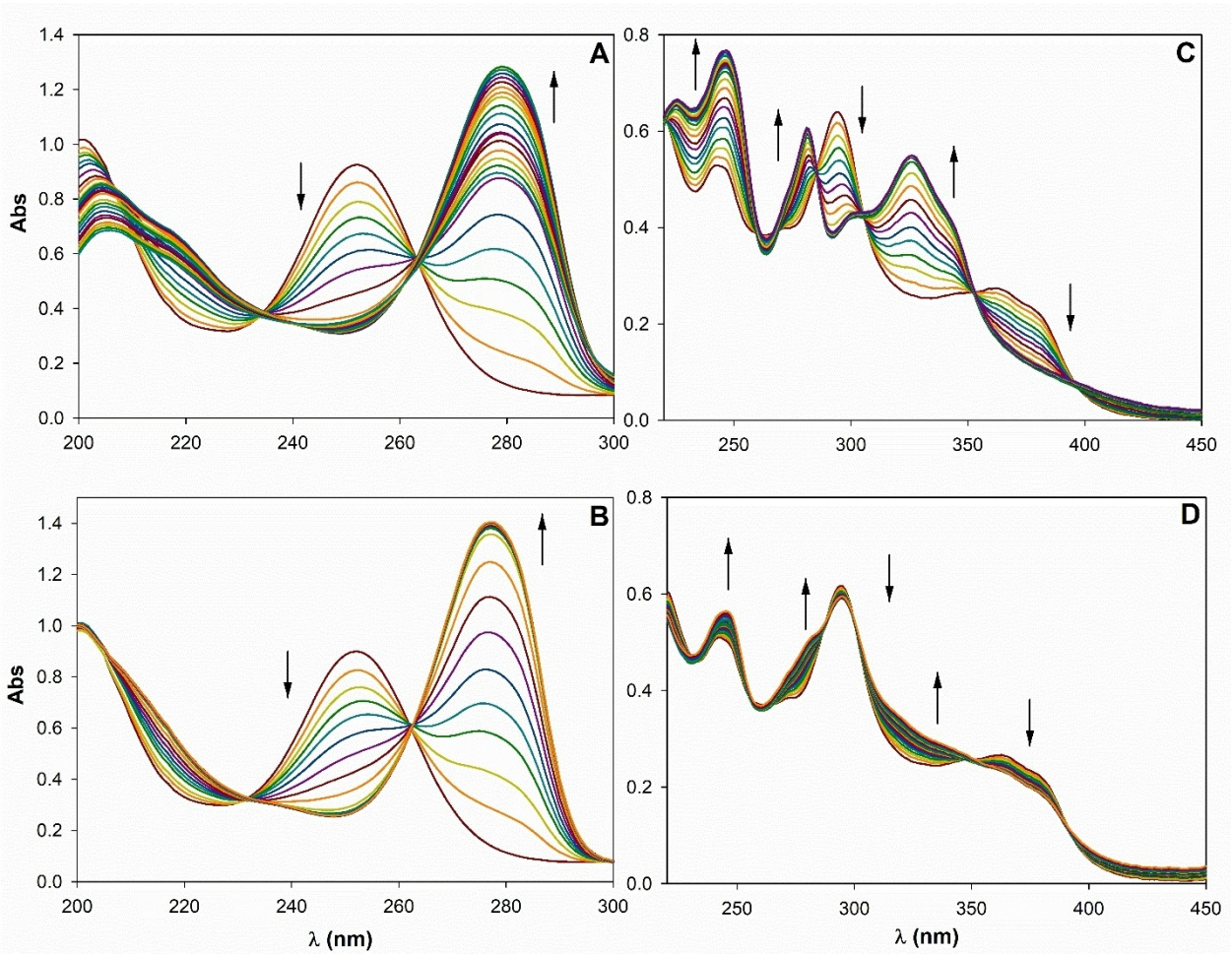

Figure 2. UV/Vis spectra of $Tre(HQ)_2$ (2.0×10^{-5} M) upon addition of A) $Cu(ClO_4)_2$ (0–2.5 mol equiv), B) $ZnCl_2$ (0–2.2 mol equiv) in MOPS (2 mM, pH 7.4) at 25 °C. UV/Vis spectra of $(HQ)_2$ (2.0×10^{-5} M) upon addition of C) $Cu(ClO_4)_2$ (0–2.1 mol equiv), D) $ZnCl_2$ (0–21 mol equiv) in dioxane/MOPS (2 mM, pH 7.4) 50:50 v/v at 25 °C.

by the ligand. The UV-vis spectrum of $Tre(HQ)_2$ in 3-N-morpholinopropanesulfonic acid (MOPS) buffer (pH 7.4, 20 mM) is characterized by absorption bands at 252, and 200 nm, as typically observed for HQs.[43,44] MOPS was used for the metal speciation studies as it does not significantly bind copper ions within at pH 7.4.[45] The addition of increasing concentrations of Cu^{2+} caused the formation of new bands at 279 and 204 nm (Figure 2A). Analyzing in-depth, the molar ratio graph (Abs vs M/L) at 279 nm, significant spectral changes were observed from 0.1 to 2.5 mol equiv. of Cu^{2+}, as the result of the Cu complexation (Figure S2). A net inflection was observed at an M/L ratio of 1:1, suggesting the formation of a main CuL species (Figure S2). However, the variation of the absorbance at 279 nm up to an M/L ratio of 2.5:1 suggested that a Cu_2L species is formed in the presence of an excess of Cu. CD spectra were also recorded in the presence of increasing concentrations of Cu^{2+} (Figure S1). Besides the positive band at 218 nm, the appearance of exciton bands at 269 and 287 nm suggested an arrangement of quinoline residues resulting from the Cu^{2+} complexation. The CD spectral changes corroborate the UV data (Figure S3), supporting the formation of more metal complex species, namely CuL and Cu_2L. ESI-MS was also used to determine the stoichiometry of the complex species. The identification of the complex species was obtained by analyzing their *m/z* value and the isotopic pattern of the peaks. The ESI-MS experiments, performed at 1:1, 1:2, and 2:1 metal-to-ligand (M/L) ratios and pH 7, revealed that CuL is the main species over the explored ratios. L is a hydroxyquinolinate derivative in which the phenolic OH groups are deprotonated. ML species appears as singly charged adduct with a proton ion $[CuL+H]^+$ at an *m/z* 744.3 with the isotopic pattern in agreement with the simulated pattern for the molecular composition $C_{32}H_{33}CuN_4O_{13}$ (see Table S1, Figure S7). However, dinuclear copper species were also detected in ESI-MS experiments only at a 2:1 M/L ratio.

Through the analysis of the data and the comparison with analogous HQs, we can hypothesize a tetradentate N_2O_2 CuL complex species for $Tre(HQ)_2$ ($2N_{pyridine}$ and $2O_{phenolate}$).[34,36] In the Cu_2L, the deprotonation of the amide groups could be hypothesized in the presence of Cu^{2+}, as previously observed for other similar derivatives.[36]

The Zn^{2+}-binding capacity of $Tre(HQ)_2$ was also investigated at 25 °C in buffered solutions (pH 7.4, MOPS). The titration with Zn^{2+} significantly influenced the UV and CD spectra of the ligand, leading to the formation of new bands (Figure 2B and Figure S4). The intensity of these bands increased up to the addition of approximately one Zn^{2+} mol equiv, suggesting the formation of a ZnL species. Furthermore, the presence of clear isosbestic points at 231 and 262 nm in the UV spectra and 245 and 278 nm in the CD spectra, also indicated that the ligand can form only one complex species at physiologic pH value. The plots of absorbance at 277 nm and molar ellipticity at 285 nm versus the Zn^{2+}/L ratio confirm that the stoichiometry of the formed complex is M/L 1:1 as the break in the slope of the curve is evident at M/L = 1 (Figure S5 and Figure S6). ESI-MS spectra confirm UV and CD data showing at all ratios only a signal attributable to the formation of a zinc complex species, namely $[ZnL+H]^+$ at m/z 745.3 (Figure S8). The coordination of the amide groups for the formation of a Zn_2L species can be excluded based on the obtained data and for comparison with other HQ glycoconjugates[47]. In keeping with the Irving-Williams series, $Tre(HQ)_2$ binds Cu^{2+} with a higher affinity compared to Zn^{2+} as further demonstrated by displacement experiments (Figure S11 and Figure S12). Upon the addition of 6 equivalents of Zn^{2+} to a $Cu^{2+}/Tre(HQ)_2$ 1:1 solution, UV and CD spectra showed that Cu^{2+} was only partially displaced. The spectra of the mixture $Cu^{2+}/Tre(HQ)_2/Zn^{2+}$ 1:1:6 is not superimposable to that of $Tre(HQ)_2/Zn^{2+}$ 1:1. However, $Tre(HQ)_2$ cannot be considered very selective for Cu^{2+} as few equivalents of Zn^{2+} can partially displace Cu^{2+} from the complex.

When an $(HQ)_2$ solution is titrated with Cu^{2+}, hyperchromic and bathochromic shifts of the bands centered around 242 nm, the appearance of the bands at 281 and 326 nm and the disappearance of the bands at 294 and 364 nm were observed in the UV spectra (Figure 2C) in dioxane/MOPS (2 mM, pH 7.4) 50:50 v/v. Unlike $Tre(HQ)_2$, $(HQ)_2$ showed clear isosbestic points in the spectra upon the addition of Cu^{2+}, in keeping with the formation of one complex species. The molar ratio graph at 326 nm revealed a marked inflection at Cu^{2+}/L 1:1, whereas no further changes were observed when an excess of Cu^{2+} was added. At a higher M/L ratio than 1, the spectra did not change significantly (Figure S13). As for ESI-MS data obtained in methanol/water 50:50 v/v (pH 7), only copper complex species were detected when a $Cu^{2+}/(HQ)_2$ solution at different ratios was injected in the MS-spectrometer. The peaks due to species CuL with different ions adducts such as $[CuL+H]^+$, $[CuL+Na]^+$ were revealed, along with cluster species $[Cu_2L_2+H]^+$ and $[Cu_2L_2+Na]^+$ (Table S1), that could be a result of the ESI process. Overall, these data and the comparison with similar metal-binding compounds[48–50] suggest the formation of the CuL species with an N_2O_2 coordination environment. Unlike $Tre(HQ)_2$, $(HQ)_2$ can form only a complex species, the presence of more potential donor atoms in $Tre(HQ)_2$ compared to $(HQ)_2$ explains this different behavior.

No significant shifts in the UV spectra were observed with Zn^{2+} (Figure 2D) in the same assay conditions of the Cu^{2+} titration. In the presence of an excess of Zn^{2+}, slight changes were observed in the UV spectrum (Figure 2D). Indeed, the complexation of Zn^{2+} by $(HQ)_2$ is promoted at higher temperature and pH.[51] As for MS data, peaks attributable to ZnL species and its clusters were detected in addition to the peaks assigned to the ligand ion adducts $[LH_2+H]^+$, $[LH_2+Na]^+$ that were the main peaks.

The addition of 100 equivalents of Zn^{2+} to a $Cu^{2+}/(HQ)_2$ 1:1 solution did not affect the Cu complexation in the assay conditions (Figure S14). These results indicate that $(HQ)_2$ is a specific ligand of Cu^{2+}. Since the ionic radii of divalent transition metal ions fall within 0.7–0.8 Å and both Cu^{2+} and Zn^{2+} can bind to N and O donor atom containing ligands, having a selective Cu^{2+} chelator is a significant coordination chemistry challenge.

Moreover, $(HQ)_2$ can extract Cu^{2+} ions from $Tre(HQ)_2$. As observed in Figure S15, the addition of 1 equiv. of $(HQ)_2$ to a $Cu^{2+}/Tre(HQ)_2$ solution caused the disappearance of the CD

signals attributable to the Cu^{2+} complex of $Tre(HQ)_2$. Only the bands due to the free ligand $Tre(HQ)_2$ are evident, suggesting the total displacement of $Tre(HQ)_2$ and the formation of 100% Cu^{2+}-$(HQ)_2$ complex. These data suggest that $(HQ)_2$ can bind Cu^{2+} ions with a much higher affinity compared to $Tre(HQ)_2$.

Interaction of the ligands with Cu-Aβ species. We performed a series of experiments to evaluate the ability of bisHQs to retrieve Cu^{2+} from the Cu^{2+}-$A\beta_{16}$ system in the presence and absence of Zn^{2+}.These experiments are typically performed with different techniques,[18,20] we used UV and CD spectroscopy. $A\beta_{16}$ was used in these experiments as it is a soluble and stable model compound of the most common Aβ forms. $A\beta_{16}$ contains the N-terminal region involved in the metal-binding sites.

BisHQs were added to a Cu^{2+}-$A\beta_{16}$ solution at equimolar concentrations. The spectra of Cu^{2+}-bisHQs and Cu–$A\beta_{16}$-bisHQs are similar (Figure 3A), also in the presence of 1 equiv. of Zn^{2+} (Figure S16 and S17). These data suggest that bisHQs can remove the Cu^{2+} ion from $A\beta_{16}$ both in the presence and in the absence of Zn^{2+}. In particular, $(HQ)_2$ can extract Cu^{2+} in the presence of an excess of Zn^{2+} (Figure S16).

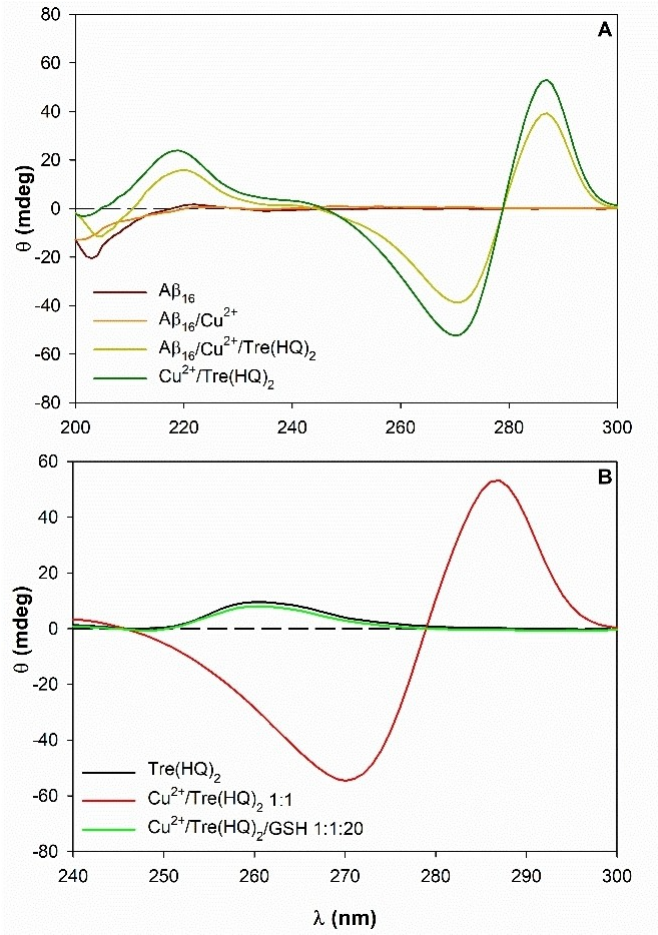

Figure 3. CD spectra of the mixtures A) Cu^{2+}/$Tre(HQ)_2$ 1:1, Cu/$A\beta_{16}$/$Tre(HQ)_2$ 1:1:1, $A\beta_{16}$ alone and Cu^{2+}/$A\beta_{16}$. $[Tre(HQ)_2] = 20\ \mu M$, $[A\beta_{16}] = 20\ \mu M$, $[Cu^{2+}] = 20\ \mu M$, MOPS (2 mM, pH 7.4), cuvette path length = 1 cm; B) $Tre(HQ)_2$ alone, Cu^{2+}/$Tre(HQ)_2$ 1:1, Cu^{2+}/$Tre(HQ)_2$/GSH 1:1:20. $[Tre(HQ)_2] = 20\ \mu M$, $[GSH] = 400\ \mu M$, $[Cu^{2+}] = 20\ \mu M$, MOPS (2 mM, pH 7.4), cuvette path length = 1 cm.

We also evaluated the ability of bisHQs to extract Cu^{2+} ions, inhibiting the Cu^{2+}-mediated aggregation of Aβ through turbidity measurements at 405 nm (Figure 4A). Equimolar solutions of Aβ and Cu^{2+} in the presence or absence of bisHQs and other reference compounds (EDTA, Trehalose (Tre), HQ) were monitored. Figure 4A shows that Cu^{2+} significantly induced Aβ aggregation and the addition of EDTA caused a significant reduction in Cu^{2+}-induced aggregation, as expected since EDTA chelates Cu^{2+}. Unlike EDTA, Tre did not affect the Cu^{2+}-mediated Aβ aggregation because it cannot bind Cu^{2+} at physiological pH. BisHQs inhibit the Cu^{2+}-mediated aggregation, and the inhibition efficiency is much higher than that of HQ. This behavior can be explained by the ability of the ligands to extract Cu^{2+} from Cu^{2+}-Aβ species. $(HQ)_2$ exhibited the greatest ability to inhibit the aggregation, and such effect is due to the higher affinity of $(HQ)_2$ for Cu^{2+} compared to Tre $(HQ)_2$ as demonstrated by the displacement experiments.

Interaction of the copper complexes with GSH. Since GSH acts as a physiological intracellular reducing agent of Cu^{2+} and provides the released Cu^{+} to Cu enzymes, the release of Cu from Cu^{2+}-bisHQs in the presence of GSH was also investigated (Figure 3B, Figure S18, and Figure S19). We monitored the demetallation of Cu^{2+}-bisHQs by UV and CD spectroscopy in the presence of GSH at physiological pH. Upon addition of 20 mol equiv. of GSH, $Tre(HQ)_2$ is completely demetalated whereas the $(HQ)_2$ released the Cu at higher mol equivalents of GSH (Figure S18 and Figure S19). Therefore, bisHQs can extract Cu^{2+} from Cu–Aβ and released it in the presence of an excess of GSH (GSH reaches the concentration of 1–10 mM in cells).

Ascorbate consumption. To investigate the use of bisHQs as drug candidates, the specific reactivity of the corresponding copper complexes was also evaluated. A major issue is the potential ability of these complexes to generate ROS in the presence of a biological reducing agent. For this reason, the redox inertness of copper complexes for potential anti-neurodegenerative drugs is often assessed.[38,52]

ROS production of Cu complexes of bisHQs was evaluated through kinetics of ascorbate (AA) oxidation, monitored by UV spectroscopy (Figure S20). The studies were also performed in the presence of Zn^{2+} to mimic the AD brain conditions, as reported in other studies.[20,39]

The rate (V_0) of the AA consumption is reported in Figure 4B, Figure 4C, and is strictly related to the ROS formation. To rule out any possible interferences from slow Cu^{2+} kinetic complexation, the ascorbate consumption experiments were also carried out adding ligands or complexes during the time course (Figure S21).

The autoxidation of AA in HEPES at pH 7.4 is very low, as suggested by the trend of absorbance at 265 nm and the V_0 value (Figure S18 and Figure 4B). When Cu^{2+} is added, the absorbance at 265 nm rapidly decreased according to the rapid AA oxidation catalyzed by Cu^{2+} (Figure S18). We first studied the ability of copper complexes of bisHQs to generate ROS in the presence of an excess of AA. Furthermore, we evaluated the

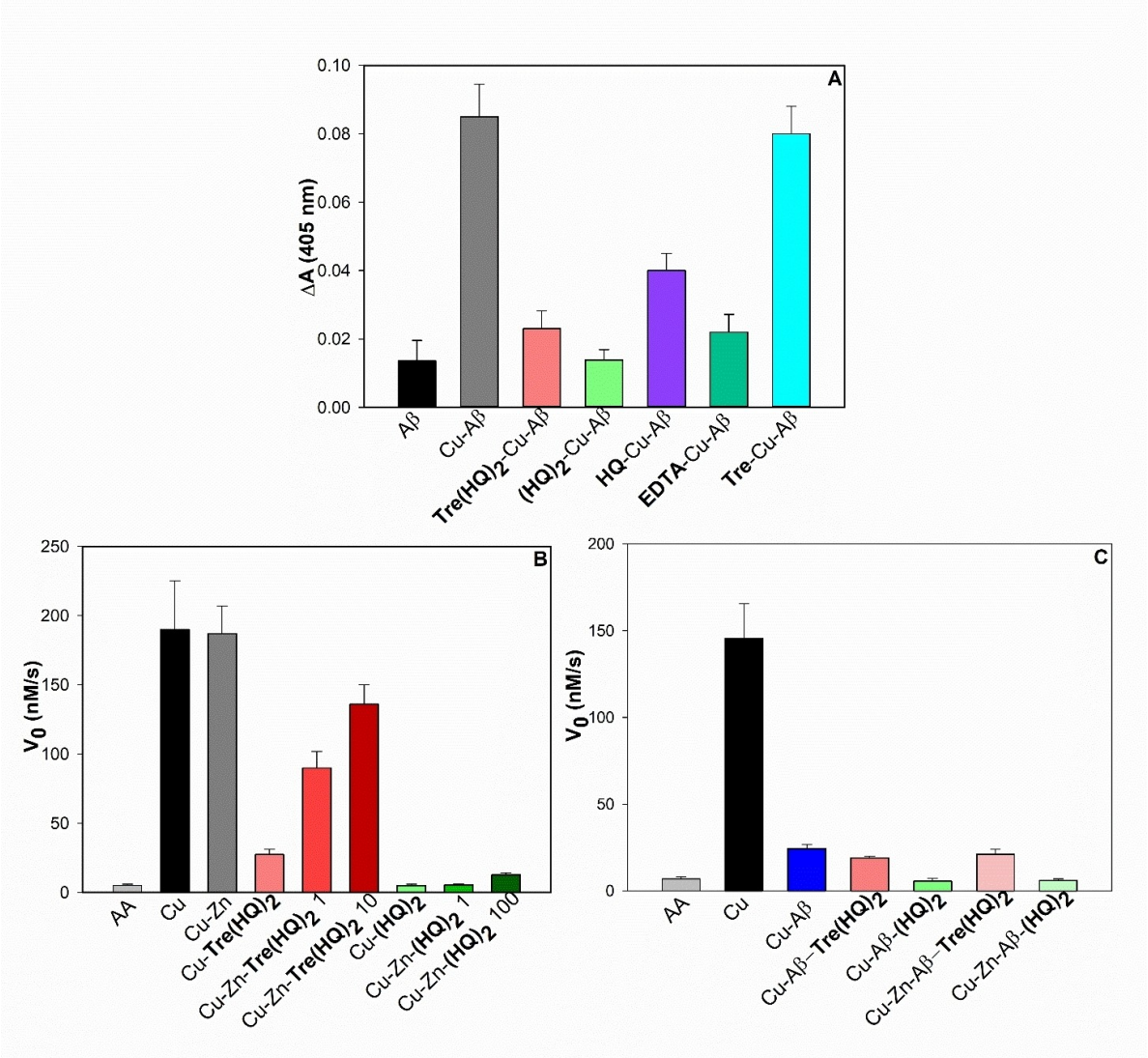

Figure 4. A)Turbidity of Aβ (2×10^{-5} M) solutions (black bar) with Cu^{2+} ions (2×10^{-5} M) in the absence (grey bar) and presence of the tested compounds (4×10^{-5} M, other colors) after incubation at 37 °C in HEPES (20 mM, pH 6.6) for 3 h. B) Initial oxidation reaction rate (V_0) of AA alone and in the presence of Cu alone, Cu complexes of HQ derivatives (Cu-Tre$(HQ)_2$ and Cu-$(HQ)_2$), a mixture of Cu^{2+}, Zn^{2+} at a 1:1 ratio (Cu–Zn), mixtures of Cu–Zn-Tre$(HQ)_2$ and Cu–Zn-$(HQ)_2$ with 1, 10 or 100 mol equiv. of Zn^{2+} compared to Cu^{2+}. The rate was measured at 25 °C with [AA] = 100 μM, $[Cu^{2+}]=2.0\times10^{-6}$ M, [ligand] = 4.0×10^{-6} M, in HEPES buffer (50 mM, pH 7.4). C) V_0 of AA in the presence of Cu alone, Cu–$A\beta_{28}$, and mixtures of Cu–$A\beta_{28}$-bisHQs Cu–Zn–$A\beta_{28}$-bisHQs. The rate was measured at 25 °C with [AA] = 100 μM, $[Cu^{2+}]=2.0\times10^{-6}$ M, $[Zn^{2+}]=2.0\times10^{-6}$ M, [ligand] = 4.0×10^{-6} M, [Aβ] = 4.0×10^{-6} M in HEPES buffer (50 mM, pH 7.4). ΔA and V_0 values are the average of three independent measurements, and the error bars represent standard deviations.

effects of Zn^{2+} on the ability of bisHQs to prevent ROS production.

The Cu^{2+} complexes of bisHQs show a smaller oxidation rate V_0, hence they have a lower catalytic activity compared to free Cu (Figure 4B).

Tre$(HQ)_2$ can reduce the reductive activation of dioxygen by Cu^{2+} in the presence of 1 mol equiv. and 10 mol equiv. of Zn^{2+}, but less efficiently than in absence of Zn^{2+} (Figure 4B). Unlike Tre$(HQ)_2$, $(HQ)_2$ can completely suppress the in vitro aerobic oxidation of AA even in the presence of 1 and 100 mol equiv. of Zn^{2+} compared to Cu^{2+} (Figure 4B). These effects can be related to higher selectivity of $(HQ)_2$ for Cu^{2+} compared to Zn^{2+} and therefore, $(HQ)_2$ has the potential to stop ROS production in a Zn^{2+}-rich AD-like environment. Since the catalytic activity of Cu bound to Aβ leads to the ROS formation contributing to the oxidative stress observed in AD, the ascorbate consumption was also monitored in the presence of Cu–Aβ species and Cu-Zn–Aβ species (Figure S21 and Figure S22). As reported in Figure S22, the addition of Cu–Aβ to an AA solution, causes a reduction of the oxidation rate of AA compared to that of Cu^{2+} alone. When $(HQ)_2$ or Zn-$(HQ)_2$ was added to a Cu–Aβ solution, the oxidation rate was similar to that of autooxidation of AA. Overall, upon the addition of bisHQs to an Aβ–Cu solution, the oxidation rate (V_0) of AA, was statistically equivalent to that found with the Cu^{2+}-complexes of bisHQs both in the presence of absence of 1 equiv. of Zn^{2+}(Figure 4C). This finding is

consistent with the ability of bisHQs to extract Cu^{2+} from Aβ. Moreover, the effects of the ligands remained unchanged also in the presence of Cu-Zn–Aβ species, suggesting once again the ability to bisHQs to target Cu also in the presence of Zn^{2+}.

Conclusions

Since metal ions are considered to be involved in the etiology of neurodegenerative disorders, numerous metal-binding agents have been proposed as potential drug candidates in AD. Nevertheless, the lack of successful clinical outcomes of most tested chelating agents highlights the importance to evaluate new ligands that meet specific requirements as reviewed elsewhere.[22] 6,6′-Dideoxy-6,6′-di[(8-hydroxyquinoline)-2-carboxyl]amino]-α,α′-trehalose (Tre$(HQ)_2$), N-butyl-2,2-imino-bis (8-hydroxyquinoline) ($(HQ)_2$) have shown the ability to extract copper ions from Aβ species and inhibit ROS formation. In particular, N-butyl-2,2′-imino-bis(8-hydroxyquinoline) is the most promising compound as it can selectively target Cu–Aβ reactivity in the presence of Zn^{2+} ions such as in AD brain patients and contribute to restoring Cu homeostasis. Moreover, $(HQ)_2$ fulfills the criteria of drug-likeness (Lipinski's rule-of-five and Veber's rule). Overall, $(HQ)_2$ satisfies important properties for the development of better ligands in the context of AD such as Cu chelation, redox inertness, selectivity, stability, and drug-likeness properties.

Experimental Section

Chemicals and Materials. Commercially available reagents such as N-butyl-2,2′-imino-bis(8-hydroxyquinoline) $(HQ)_2$, glutathione (GSH), ascorbate (AA) were obtained from Sigma-Aldrich. Tre$(HQ)_2$ was synthesized as reported elsewhere.[40] Stock solutions of Cu^{2+} and Zn^{2+} salts (perchlorate or chloride) were prepared by dissolving the corresponding salt in water and titrating the resulting solutions with standardized EDTA using murexide and eriochrome black T, respectively.

UV-visible and circular dichroism spectroscopy. UV-vis spectra were recorded on an Agilent 8452 A diode array spectrophotometer whereas CD experiments were performed on a JASCO spectropolarimeter (model J-1500) endowed with a Peltier temperature controller. All UV and CD measurements were performed using cuvettes with a path length of 1 cm. The CD spectra represent the average of at least 5 scans. Metal coordination studies were carried out in buffer at pH 7.4, the metal complexes of $(HQ)_2$ were less soluble than those of Tre$(HQ)_2$ and the addition of an organic solvent (dioxane) was required in the UV titrations of $(HQ)_2$ with Cu^{2+}.

Mass Spectrometry. ESI-MS experiments were performed on a Finnigan LCQ DECA XP PLUS ion trap spectrometer operating in the positive ion mode and equipped with an orthogonal ESI source (Thermo Electron Corporation, USA).

Sample solutions of metal complexes diluted with ultrapure water and/or methanol were injected into the ion source using nitrogen as the drying gas. The pH of the sample solutions was adjusted with NaOH at pH 7.4.

Copper(II) and zinc(II) complexes for ESI-MS studies were prepared by adding a solution of copper(II) or zinc(II) to a ligand water solution of Tre$(HQ)_2$ and water/methanol solution of $(HQ)_2$. Different metal-ligand ratios were investigated. Sample solutions were injected into the ion source at a flow rate of 5 μL/ min. The mass spectrometer operated with a capillary voltage of 46 V and a capillary temperature of 275 °C, while the spray voltage was 4.3 kV.

The assignments of the peaks in ESI-MS spectra were performed through Xcalibur software comparing the experimental isotopic patterns with the corresponding simulated profiles. Each species is indicated with the m/z value of the first peak of the isotopic cluster.

Aβ preparation. $Aβ_{1-40}$ peptide was obtained from Bachem (Bubendorf, Switzerland) and dissolved in ammonium hydroxide (2%). Such solvent was removed by lyophilization and $Aβ_{1-40}$ was then dissolved in NaOH (1 mM), sonicated, and then buffered (pH 7.4), and diluted to the desired peptide concentration. $Aβ_{1-16}$ and $Aβ_{1-28}$ were also purchased from Bachem, directly dissolved in buffer, and used as models of amyloid peptides as they contain the metal coordination site of Aβ and do not precipitate in the presence of metal ions.

Cu-mediated Aβ aggregation assay. The turbidity assay allowed us to evaluate the ability of bisHQs to inhibit the aggregation triggered by Cu^{2+}, extracting Cu^{2+} from Aβ. All solutions were obtained using a chelex-treated HEPES buffer (20 mM, pH 6.6). The pH (6.6) of the buffer was utilized because Cu^{2+} strongly induced the aggregation of $Aβ_{1-40}$ at this pH,[53] and acidosis may play a role in the AD brain.[54] Stock solutions of agents such as EDTA, 8-hydroxyquinoline (HQ), and trehalose (Tre) were prepared in water and diluted with HEPES buffer. The solutions were incubated for 3 h at 37 °C and absorbance (Abs) measured at 405 nm. Turbidity (ΔA) was obtained by the difference in absorbance at 405 nm between the sample and its corresponding control that did not contain Aβ. The molar ratio between $Aβ_{1–40}$ (20 μM), metal ion, and ligand, was 1 : 1 : 2. All experiments were performed in triplicate. Both Cu^{2+} and $Aβ_{1-40}$ were positive controls to demonstrate the effect on peptide aggregation in the absence of the ligands.

Ascorbate (AA) oxidation assay. AA oxidation was monitored by measuring the absorbance at $\lambda = 265$ nm (unoxidized AA) in HEPES buffer (50 mM, pH 7.4) as reported elsewhere.[55,56] Free Cu^{2+} or Cu^{2+}-complexes were added ($[Cu^{2+}] = 2.0$ μM, [ligand] = 2.0 μM or 4.0 μM) to the AA solution (100 μM) inside the cuvette (1 cm). Kinetic measurements of AA oxidation were performed in triplicate with independent daily fresh prepared solutions. The molar AA oxidation rate (nM/s) was obtained by dividing the initial slope of Abs_{265} vs time (s) by the extinction coefficient of AA ($\varepsilon_{265} = 14500\ M^{-1}cm^{-1}$). The absorbance of the Cu complexes (at $\lambda =$ 265 nm) in the same conditions were used as blank even if it was negligible.

Acknowledgments

We thank the Università degli Studi di Catania (Piano di incentivi per la ricerca di Ateneo 2020/2022 Pia.ce.ri.), the Italian Ministero dell'Università e della Ricerca for the financial support.

Conflict of Interest

The authors declare no conflict of interest.

Keywords: Copper · Amyloid · Zinc · Quinoline · Trehalose

[1] *Alzheimer's Dement.* **2019**, *15*, 321–387.
[2] *Alzheimer's Dement.* **2020**, *16*, 391–460.
[3] C. Cheignon, M. Tomas, D. Bonnefont-Rousselot, P. Faller, C. Hureau, F. Collin, *Redox Biol.* **2018**, *14*, 450–464.
[4] V. Oliveri, *Eur. J. Med. Chem.* **2019**, *167*, 10–36.
[5] E. Atrián-Blasco, P. Gonzalez, A. Santoro, B. Alies, P. Faller, C. Hureau, *Coord. Chem. Rev.* **2018**, *371*, 38–55.
[6] M. Rana, A. K. Sharma, *Metallomics* **2019**, *11*, 64–84.
[7] E. Carboni, P. Lingor, *Metallomics* **2015**, *7*, 395–404.
[8] H. Kozlowski, M. Luczkowski, M. Remelli, D. Valensin, *Coord. Chem. Rev.* **2012**, *256*, 2129–2141.
[9] M. G. Savelieff, G. Nam, J. Kang, H. J. Lee, M. Lee, M. H. Lim, *Chem. Rev.* **2018**, *119*, 1221–1322.
[10] C. Rodríguez-Rodríguez, M. Telpoukhovskaia, C. Orvig, *Coord. Chem. Rev.* **2012**, *256*, 2308–2332.
[11] P. Faller, C. Hureau, *Dalton Trans.* **2009**, 1080–1094.
[12] K. P. Kepp, *Coord. Chem. Rev.* **2017**, *351*, 127–159.
[13] M. A. Lovell, J. D. Robertson, W. J. Teesdale, J. L. Campbell, W. R. Markesbery, *J. Neurol. Sci.* **1998**, *158*, 47–52.
[14] E. Nam, G. Nam, M. H. Lim, *Biochemistry* **2020**, *59*, 15–17.
[15] T. Branch, M. Barahona, C. A. Dodson, L. Ying, *ACS Chem. Neurosci.* **2017**, *8*, 1970–1979.
[16] P. Ghosh, G. Maayan, *Chem. Sci.* **2020**, *11*, 10127–10134.
[17] A. Rakshit, K. Khatua, V. Shanbhag, P. Comba, A. Datta, *Chem. Sci.* **2018**, *9*, 7916–7930.
[18] E. Atrián-Blasco, A. Conte-Daban, C. Hureau, *Dalton Trans.* **2017**, *46*, 12750–12759.
[19] A. Conte-Daban, A. Day, P. Faller, C. Hureau, *Dalton Trans.* **2016**, *45*, 15671–15678.
[20] C. Esmieu, R. Balderrama-Martínez-Sotomayor, A. Conte-Daban, O. Iranzo, C. Hureau, *Inorg. Chem.* **2021**, *60*, 1248–1256.
[21] S. Ayala, P. Genevaux, C. Hureau, P. Faller, *ACS Chem. Neurosci.* **2019**, *10*, 3366–3374.
[22] C. Esmieu, D. Guettas, A. Conte-Daban, L. Sabater, P. Faller, C. Hureau, *Inorg. Chem.* **2019**, *58*, 13509–13527.
[23] V. Oliveri, *Coord. Chem. Rev.* **2020**, *422*, DOI 10.1016/j.ccr.2020.213474.
[24] A. Robert, Y. Liu, M. Nguyen, B. Meunier, *Acc. Chem. Res.* **2015**, *48*, 1332–1339.
[25] P. A. Adlard, R. A. Cherny, D. I. Finkelstein, E. Gautier, E. Robb, M. Cortes, I. Volitakis, X. Liu, J. P. Smith, K. Perez, K. Laughton, Q. X. Li, S. A. Charman, J. A. Nicolazzo, S. Wilkins, K. Deleva, T. Lynch, G. Kok, C. W. Ritchie, R. E. Tanzi, R. Cappai, C. L. Masters, K. J. Barnham, A. I. Bush, *Neuron* **2008**, *59*, 43–55.
[26] C. Grossi, S. Francese, A. Casini, M. C. Rosi, I. Luccarini, A. Fiorentini, C. Gabbiani, L. Messori, G. Moneti, F. Casamenti, *J. Alzheimer's Dis.* **2009**, *17*, 423–440.
[27] J. Toyn, *Expert Rev. Clin. Pharmacol.* **2015**, *8*, 267–269.
[28] F. Mesiti, D. Chavarria, A. Gaspar, S. Alcaro, F. Borges, *Eur. J. Med. Chem.* **2019**, *181*, DOI 10.1016/j.ejmech.2019.111572.
[29] D. Knez, N. Coquelle, A. Pišlar, S. Žakelj, M. Jukič, M. Sova, J. Mravljak, F. Nachon, X. Brazzolotto, J. Kos, J. P. Colletier, S. Gobec, *Eur. J. Med. Chem.* **2018**, *156*, 598–617.
[30] X. Yang, P. Cai, Q. Liu, J. Wu, Y. Yin, X. Wang, L. Kong, *Bioorg. Med. Chem.* **2018**, *26*, 3191–3201.
[31] V. Oliveri, G. Vecchio, *Eur. J. Med. Chem.* **2016**, *120*, 252–274.
[32] V. Oliveri, F. Bellia, G. Vecchio, *Chem. Eur. J.* **2017**, *23*, 4442–4449.
[33] V. Oliveri, F. Bellia, G. Vecchio, *ChemistrySelect* **2017**, *2*, 655–659.
[34] V. Oliveri, F. Bellia, A. Pietropaolo, G. Vecchio, *Chem. Eur. J.* **2015**, *21*, 14047–14059.
[35] V. Oliveri, *ChemistryOpen* **2015**, *4*, 792–795.
[36] V. Oliveri, C. Sgarlata, G. Vecchio, *Chem. Asian J.* **2016**, *11*, 2436–2442.
[37] M. Nguyen, C. Bijani, N. Martins, B. Meunier, A. Robert, *Chem. Eur. J.* **2015**, *21*, 17085–17090.
[38] M. Nguyen, A. Robert, A. Sournia-Saquet, L. Vendier, B. Meunier, *Chem. Eur. J.* **2014**, *20*, 6771–6785.
[39] W. Zhang, Y. Liu, C. Hureau, A. Robert, B. Meunier, *Chem. Eur. J.* **2018**, *24*, 7825–7829.
[40] V. Oliveri, F. Bellia, G. I. Grasso, A. Pietropaolo, G. Vecchio, *RSC Adv.* **2016**, *6*, 47229–47236.
[41] S. Bastianetto, S. Krantic, R. Quirion, *Mini-Rev. Med. Chem.* **2008**, *8*, 429–435.
[42] V. Oliveri, S. Zimbone, M. L. Giuffrida, F. Bellia, M. F. Tomasello, G. Vecchio, *Chem. Eur. J.* **2018**, *24*, 6349–6353.
[43] C. Sgarlata, V. Oliveri, J. Spencer, *Eur. J. Inorg. Chem.* **2015**, 5886–5891.
[44] V. Oliveri, F. Attanasio, A. Puglisi, J. Spencer, C. Sgarlata, G. Vecchio, *Chem. Eur. J.* **2014**, *20*, 8954–8964.
[45] H. E. Mash, Y. P. Chin, L. Sigg, R. Hari, H. Xue, *Anal. Chem.* **2003**, *75*, 671–677.
[46] V. Oliveri, A. Puglisi, M. Viale, C. Aiello, C. Sgarlata, G. Vecchio, J. Clarke, J. Milton, J. Spencer, *Chem. Eur. J.* **2013**, *19*, 13946–13955.
[47] V. Oliveri, A. Pietropaolo, C. Sgarlata, G. Vecchio, *Chem. Asian J.* **2017**, *12*, 110–115.
[48] C. Deraeve, A. Maraval, L. Vendier, V. Faugeroux, M. Pitié, B. Meunier, *Eur. J. Inorg. Chem.* **2008**, 5622–5631.
[49] C. Deraeve, M. Pitié, H. Mazarguil, B. Meunier, *New J. Chem.* **2007**, *31*, 193–195.
[50] C. Deraeve, C. Boldron, A. Maraval, H. Mazarguil, H. Gornitzka, L. Vendier, M. Pitié, B. Meunier, *Chem. Eur. J.* **2008**, *14*, 682–696.
[51] P. Murer, S. Allenbach, G. Wagenblast, C. Schildknecht, C. Lennartz, *Metal Complexes with Dibenzo[f,h]Quinoxalines.* **2013**.
[52] M. Nguyen, B. Meunier, A. Robert, *Eur. J. Inorg. Chem.* **2017**, *2017*, 3198–3204.
[53] C. S. Atwood, R. D. Moir, X. Huang, R. C. Scarpa, N. M. E. Bacarra, D. M. Romano, M. A. Hartshorn, R. E. Tanzi, A. I. Bush, *J. Biol. Chem.* **1998**, *273*, 12817–12826.
[54] E. B. Gonzales, N. Sumien, *J. Alzheimer's Dis.* **2017**, *57*, 1137–1144.
[55] F. Bellia, G. I. Grasso, I. M. M. Ahmed, V. Oliveri, G. Vecchio, *Chem. Eur. J.* **2020**, *26*, 16690–16705.
[56] R. De Ricco, D. Valensin, S. Dell'Acqua, L. Casella, C. Hureau, P. Faller, *ChemBioChem* **2015**, *16*, 2319–2328.

Manuscript received: February 1, 2021
Revised manuscript received: April 14, 2021
Accepted manuscript online: April 16, 2021